



Paper-based three-dimensional electrochemical immunodevice based on multi-walled carbon nanotubes functionalized paper for sensitive point-of-care testing

Panpan Wang ^a, Lei Ge ^a, Mei Yan ^a, Xianrang Song ^b, Shenguang Ge ^c, Jinghua Yu ^{a,*}

^a Key Laboratory of Chemical Sensing & Analysis in Universities of Shandong, School of Chemistry and Chemical Engineering, University of Jinan, Jinan 250022, PR China

^b Cancer Research Center, Shandong Tumor Hospital, Jinan 250117, PR China

^c Shandong Provincial Key Laboratory of Fluorine Chemistry and Chemical Materials, University of Jinan, Jinan 250022, PR China

ARTICLE INFO

Article history:

Received 12 October 2011

Received in revised form

27 November 2011

Accepted 14 December 2011

Available online 23 December 2011

Keywords:

Electrochemical immunoassay

Lab on paper

Screen-printed electrode

Biomarker

Point-of-care testing

ABSTRACT

In this study, electrochemical immunoassay was introduced into the recently proposed microfluidic paper-based analytical device (μ PADs). To improve the performance of electrochemical immunoassay on μ PAD for point-of-care testing (POCT), a novel wax-patterned microfluidic paper-based three-dimensional electrochemical device (3D- μ PED) was demonstrated based on the multi-walled carbon nanotubes (MWCNTs) modified μ PAD. Using typical HRP-O-Phenylenediamine-H₂O₂ electrochemical system, a sandwich immunoassay on this 3D- μ PED for sensitive diagnosis of two tumor markers simultaneously in real clinical serum samples was developed with a linear range of 0.001–75.0 μ M⁻¹ for cancer antigen 125 and 0.05–50.0 ng mL⁻¹ for carcinoembryonic antigen. In addition, this 3D- μ PED can be easily integrated and combined with the recently emerging paper electronics to further develop simple, sensitive, low-cost, disposable and portable μ PAD for POCT, public health and environmental monitoring in remote regions, developing or developed countries.

© 2011 Elsevier B.V. All rights reserved.

1. Introduction

Whitesides and co-workers (Martinez et al., 2007, 2010a) firstly demonstrated a novel lab-on-a-paper systems using patterned paper as substrate, named microfluidic paper-based analytical devices (μ PADs), to combine the simplicity, portability, disposability and low-cost of paper strip tests and the multiplex analysis of the conventional lab-on-a-chip devices. It is a promising technology for point-of-care testing (POCT), public health and environmental monitoring applications in which highly sensitive methods and complex function must be combined with low-cost, rapid and simple fabrication and operation (Sia and Kricka, 2008; Whitesides, 2011). Much effort has been directed toward the development of fabrication (Abe et al., 2008; Chitnis et al., 2011; Fenton et al., 2009; Li et al., 2008; Lu et al., 2009; Martinez et al., 2008a), functionalization (Carrilho et al., 2009a; Hwang et al., 2011; Martinez et al., 2010b, 2008b; Noh and Phillips, 2010; Osborn et al., 2010) and quantitative (Delaney et al., 2011; Dungchai et al., 2009; Ornatska et al., 2011; Wang et al., 2011; Yu et al., 2011) methods for μ PADs.

Multiplexed immunoassay of biomarkers has recently attracted considerable interest due to its advantages in early screening of diseases, evaluating the extent of diseases, and monitoring the response of diseases to therapy. To date, however, the primary and scanty immunoassay for the qualitative analysis of multiplex analytes on μ PADs is colorimetric method (Cheng et al., 2010). Sensitive and quantitative immunoassay is still needed when a “yes” or “no” answer is insufficient and the level of an analyte in real biological sample is important for simple, rapid, low-cost POCT, public health and environmental monitoring. Electrochemical methods have traditionally received the major share of the attention in development of quantitative methods for μ PADs (Apilux et al., 2010; Carvalhal et al., 2010; Dungchai et al., 2009; Nie et al., 2010a, 2010b). The advantages of electrochemical methods would make electrochemical immunoassays an innately exciting strategy for building a new generation of paper-based POCT devices. To the best of our knowledge, no reports about establishing electrochemical immunoassay on μ PADs have been published.

In this work, to effectively combine the electrochemical immunoassay with μ PADs, we demonstrated a novel microfluidic paper-based three-dimensional electrochemical device (3D- μ PED) comprised of one layer of wax-patterned paper and one layer of screen-printed electrodes on a transparent polyethylene

* Corresponding author. Tel.: +86 531 82767161.

E-mail address: ujn.yujh@gmail.com (J. Yu).

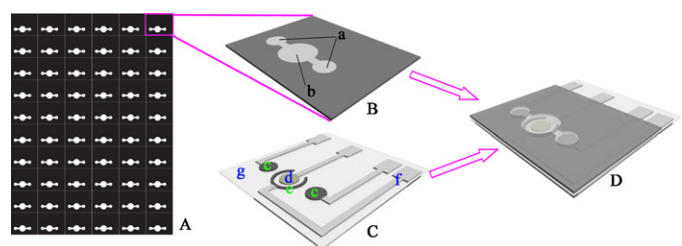
terephthalate substrate. Wax printing (Carrilho et al., 2009b), as rapid, inexpensive, insulative and particularly well-suited for producing large lots (hundreds to thousands) of prototype μ PADs, was used in this work. In this 3D- μ PED, the wax patterns on paper layer constituted reservoirs of the electrochemical cells, and the screen-printed electrodes will be connected with the aids of the wax-patterned electrochemical cells after stacking. Multi-walled carbon nanotubes (MWCNTs) (Yáñez-Sedeño et al., 2010) were used to modify the porous-structured paper working zones to enhance the electronic conductivity of the electrochemical cells on the μ PADs for the first time. The immunoreactions were performed on antibody modified paper working zones fabricated through chitosan coating and glutaraldehyde cross-linking.

The advantages of this configuration includes: (i) bulk operations of the immunoreactions and washing on paper layer will be easily realized without considering the influence, contaminate and damage to the electrodes, thus (ii) one screen-printed electrodes layer could work with one more paper layers due to the long service life of the electrodes, this could be very important for realization of low-cost POCT. Ultimately, with the aids of a simple home-made device-holder and a section-switch, the concentrations of carcinoma antigen 125 (CA125) and carcinoembryonic antigen (CEA), which showing considerable significance in early screening and clinical diagnosis of some tumor diseases (Li, 2001), in real human serum samples were simultaneously detected. This work could not only make contribution to further expand detection mode on μ PADs, but also can be easily integrated and combined with the recently emerging class of paper electronics (Tobjörk and Österbacka, 2011) to further develop integrated POCT immunodevice in our future work.

2. Experimental

2.1. Materials and reagents

Mouse monoclonal capture CA125 and CEA antibodies, HRP-labeled signal CA125, CEA antibodies and human CA125 and CEA standard solutions (0.5 mg mL^{-1}) were purchased from Shanghai Linc-Bio Science Co. Ltd. Multi-walled carbon nanotubes (MWCNTs) were purchased from Nanoport Co. Ltd. (Shenzhen, China). Chitosan and bovine serum albumin (BSA) were obtained from Sigma-Aldrich Chemical Co. (St. Louis, MO). Glutaraldehyde (25% aqueous solution) was purchased from Alfa Aesar China Ltd. O-Phenylenediamine and H_2O_2 used as electrochemical system were from Shanghai Biochemical Reagent Company (China). Whatman chromatography paper 1# ($200 \text{ mm} \times 200 \text{ mm}$) was obtained from GE Healthcare World-wide (Pudong Shanghai, China) and used with further adjustment of size. This type of Whatman paper was chosen because of its uniform composition (relative to other types of paper) and lack of additives that affect flow rate and electrochemistry reaction. The Ag/AgCl ink (CNC-01), Ag ink (737-H) and carbon ink (ED-581-SS) for screen-printed electrodes were obtained from Henkel Acheson. Ultrapure water obtained from a Millipore water purification system ($18 \text{ M}\Omega$, Milli-Q, Millipore) was used in all assays and solutions. Blocking buffer for blocking the residual reactive sites on the antibody immobilized working electrodes was 10.0 mM pH 7.4 phosphate buffer solution (PBS) containing 0.5% bovine serum albumin and 0.5% casein. To minimize unspecific adsorption, 0.05% Tween-20 was spiked into 10.0 mM pH 7.4 PBS as washing buffer. Mouse monoclonal Fluorescein isothiocyanate (FITC)-labeled signal CA125 antibodies were purchased from Shanghai Linc-Bio Science Co. Ltd. The clinical serum samples were from Shandong Tumor Hospital. All other reagents were of analytical grade and used as received.



Scheme 1. The schematic representation of this novel 3D- μ PED. (A): Wax-patterned paper sheet; (B): the 3D- μ PED, (a) paper working zones; (b) paper auxiliary zone. (C): Screen-printed electrodes, (c) carbon working electrodes; (d) Ag/AgCl reference electrode; (e) carbon counter electrode; (f) silver conductive channel and pad; (g) transparent polyethylene terephthalate substrate. (D): After stacking, the paper working zones and the paper auxiliary zone will be aligned to the screen-printed working electrodes, counter and reference electrode, respectively.

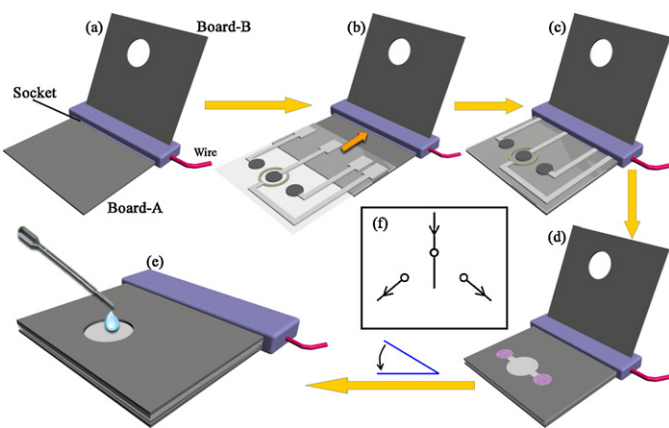
2.2. Fabrication of this 3D- μ PED

Wax was used as the paper hydrophobization and insulation agent in this work. This 3D- μ PED was comprised of two layers with the same size: one layer of wax-patterned rectangular paper and one layer of screen-printed electrodes. For wax-patterned paper layer, we designed patterns of hydrophobic barriers as black lines on a white background using Adobe illustrator CS4. The shape of the wax patterns on paper layer was shown in Scheme 1A, B. This wax-patterned paper electrochemical cell contains an paper auxiliary zone (8 mm in diameter) surrounded by two paper working zones (4 mm in diameter) with paper channels to connect them. The unprinted area constituted reservoir of electrochemical cell with a volume of $15 \mu\text{L}$. The wax-patterns were printed on paper sheet in bulk using the wax printer (Xerox Phaser 8560N color printer) set to the default parameters for photoquality printing in a high-resolution printing mode (Scheme 1A). The printer can print an A4-size paper sheet in approximately 5 s. The wax-printed paper sheet was then placed on a digital hot plate set at 150°C for 120 s, and the wax melted and penetrated through the thickness of the porous-structured paper (Fig. S2A) to form the hydrophobic patterns. The patterned paper sheet was ready for use after removing the paper sheet from the hot plate and allowing it to cool to room temperature (<10 s). The scanning electron microscopy (SEM) images of this 3D- μ PED were recorded on a JEOL JSM-5510 scanning electron microscope and shown in Supporting information. The contact angle tests were performed on contact angle measurement (Model OCA40, Dataphysics).

For screen-printed electrodes layer, as shown in Scheme 1C, the screen-printed electrodes were fabricated according to a modified previous literature (Dungchai et al., 2009). This disposable screen-printed electrodes array was comprised of two circular carbon working electrodes (4 mm in diameter), one annular carbon counter electrode and one circular Ag/AgCl reference electrode. Two working electrodes would share the same Ag/AgCl reference and carbon counter electrode after stacking (Scheme 1D). The preparation of screen-printed electrodes array was as following: the gray silver ink was firstly screen-printed on the surface of a transparent polyethylene terephthalate substrate to act as conductive channels, then the black carbon ink was screen-printed to the defined areas as the working electrodes and the counter electrode according to the shape shown in Scheme 1C. Finally the Ag/AgCl ink was printed to the defined areas as the reference electrode.

2.3. Preparation of microfluidic paper-based three-dimension electrochemical immunodevice

The preparation of microfluidic paper-based three-dimension electrochemical immunodevice (3D- μ PEID) is illustrated in



Scheme 2. Schematic representation of the facile home-made device-holder. (a) The folder-type facile device-holder; (b and c) the screen-printed electrodes was inserted into the socket; (d) paper layer was placed onto the screen-printed electrodes; (e) the device-holder was clamped closely and 10.0 mM pH 7.4 PBS buffer, containing 2.0 mM O-Phenylenediamine and 4.0 mM H₂O₂, was added, then the electrochemical reactions on each paper working zone were triggered sequentially with the aids of a section-switch; (f) circuit schematic of the section-switch.

Scheme S1(1–4). The 3D-μPEID was constructed by immobilizing the corresponding capture antibodies on the paper working zones of the wax-patterned paper through chitosan coating and glutaraldehyde cross-linking. First, 4 μL carboxylated MWCNTs (**Detail pretreatment in Supporting information**) were applied to modified paper fibers (Fig. S3B and C) in each paper working zone and dried at room temperature. Then, 3 μL of 0.25 mg mL⁻¹ chitosan (**Detail pretreatment in Supporting information**) was coated on MWCNTs modified paper fibers and dried in the air (Fig. S3D and E). After activating with 2.5% glutaraldehyde (4 μL, PBS) for 2 h and washed with PBS, 2 μL of 20 μg mL⁻¹ CA125 and CEA capture antibodies were dropped into the corresponding paper working zone (Fig. S3F), respectively, and incubated at room temperature for 25 min, subsequently, physically absorbed excess antibodies were rinsed (**Detail washing procedures in Supporting information**) with PBS and washing buffer, and a drop of 20 μL blocking buffer was applied into each paper working zone and incubated for 30 min at room temperature to block possible remaining active sites on paper fibers against nonspecific adsorption. After washing with PBS, the resulting 3D-μPEID was obtained and stored at 4 °C in a dry environment prior to use. The scanning electron microscopy (SEM) images of this 3D-μPED were recorded on a JEOL JSM-5510 scanning electron microscope and shown in **Supporting information**. Electrochemical impedance spectroscopy (EIS) was performed on a IM6x electrochemical working station (Zahner Co., Germany) and shown in **Supporting information**.

2.4. Electrochemical assay procedure of this 3D-μPEID

The electrochemical assay procedures of this 3D-μPEID were shown in **Scheme S1(5 and 6)** and **Scheme 2**, and a detailed procedure was described below. To carry out the immunoreaction and electrochemical measurement, as shown in **Scheme S1(5 and 6)**, 2 μL sample solution containing different concentration of CA125 and CEA in 10.0 mM pH 7.4 PBS was added to corresponding paper working zone and allowed to incubate for 200 s at room temperature, followed by washing with PBS and washing buffer according to the procedure mentioned in **Supporting information**. Then HRP-labeled CA125 and CEA signal antibody (2 μL, 10 μg mL⁻¹) was added to corresponding paper working zone, and allowed to incubate for 200 s at room temperature.

After being washed with PBS and washing buffer and dried again, for electrochemical assay, the 3D-μPEID was integrated

with a newly designed facile device-holder (**Scheme 2**), which was used to fix and connect the 3D-μPEID to the electrochemical detector. This folder-type device-holder was comprised of two simple circuit boards, name board-A and board-B, with a socket in it. Firstly, in detail, screen-printed electrodes layer was inserted into the socket, thus the contact pads on screen-printed electrodes layer and device-holder were connected closely. Then the paper layer was placed face-up onto the screen-printed electrodes layer to make these two layers as well as their paper working zones and screen-printed electrodes aligned. After that, the device-holder was clamped to make the 3D-μPEID stacked closely. Ultimately, 20 μL 10.0 mM pH 7.4 PBS buffer, containing 2.0 mM O-Phenylenediamine and 4.0 mM H₂O₂ were adding into the paper electrochemical cell on paper layer through the hole in board-B. With the aid of a section-switch, two working electrodes were sequentially placed into the circuit to trigger the electrochemical reaction. In the presence of HRP-labeled immunocomplexes on paper, the electroactive species, 2,2'-diaminoazobenzene (**Zhao et al., 1992**), was firstly produced. The differential pulse voltammetric (DPV) measurements were performed. The electrochemical signals were measured using a portable electrochemical workstation (PalmSens Electrochemical Portable Apparatus) at room temperature.

3. Results and discussion

3.1. Electrochemical behavior on this 3D-μPEID

The DPV responses of the glutaraldehyde/chitosan/MWCNTs modified paper working zone on the μPAD immobilized with sandwich immunocomplexes labeled with HRP in the presence of O-Phenylenediamine and H₂O₂ are shown in Fig. 1. One DPV peak appeared at about -0.57 V in the cathodic process, generated from 2,2'-diaminoazobenzene that is formed by the redox reaction of O-Phenylenediamine (**Zhao et al., 1992**). Clearly, the sandwich immunocomplexes (curve b and b' in Fig. 1A and B), in which the capture antibody was immobilized in the paper working zones of μPAD and the signal antibody was tagged with HRP, gives a much higher DPV response than the nonspecific adsorption of signal antibodies without antigen (curve a and a' in Fig. 1A and B), indicated very low levels of nonspecific adsorption of labeled signal antibodies were observed in absence of antigen. Furthermore, the DPV response increased with the increasing of the concentration of antigen (curve c and c' in Fig. 1A and B). Therefore, it could be applied to the sensitive determination of antigens in this 3D-μPEID.

3.2. Optimization of detection conditions

For paper-based POCT, the analytical cost, sensitivity and time efficiency is very important. For the analytical cost, reducing the pipetting volume of solutions into paper working zones would decrease the analytical cost remarkably by saving the immunoreagents. The detail investigation procedures were shown in **Supporting information**. Fig. 2A showed that when the pipetting volume was 2.0 μL, the uniformity and sufficiency of antibodies on the working zone was obtained. Thus, considering the analytical cost, 2.0 μL was selected as the optimal pipetting volume of all reagents. In addition, the small pipetting volume could further avoid the outflow of the solutions from paper working zones to the paper channels, this could further reduce the cross-talk between adjacent electrodes and the nonspecific adsorption of signal antibodies on the paper channels to increase the signal-to-background ratio and the sensitivity of this 3D-μPEID.

The pH of detection solution is an important factor in the enzymatic response. The effects of solution pH on the DPV responses

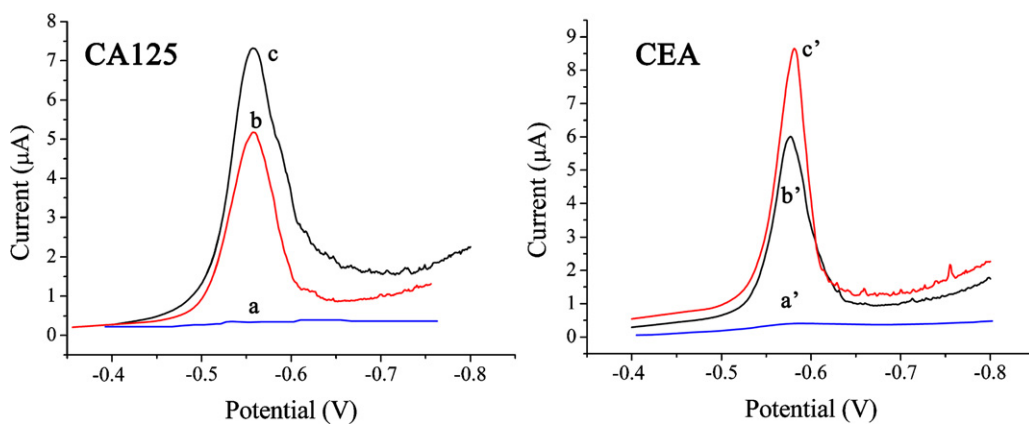


Fig. 1. DPV curves of CEA and CA125: (a and a') background without antigens; (b and b') after a sandwich immunoreaction with 2.5 U mL^{-1} CEA/ 2.5 ng mL^{-1} CA125 and (c and c') 5.0 U mL^{-1} CEA/ 5.0 ng mL^{-1} CA125.

to CA125 and CEA were investigated. Both the responses increased with the increasing pH value from 6 to 7.4 and then decreased when the pH was over 7.4. Thus, pH 7.4 PBS was selected for preparation of the detection solution.

The incubation time is an important parameter affecting the analytical performance and time efficiency of POCT. At room temperature, the DPV responses increased with the increasing incubation time used in sandwich-type immunoassay and then leveled off, which indicated a saturated binding in the immunoreaction (Fig. 2B). The optimal incubation time of CA125 immunocomplexes and CEA immunocomplexes was 150 s and 200 s, respectively. A successful development of the multiplex immunoassay required that the common incubation time must be suitable for all analytes. Thus, an incubation time of 200 s was selected in the further study. The incubation process on this 3D- μ PEID needed shorter time compared with 1–3 h at 37°C for the traditional electrochemical immunoassay. This is partly due to the high surface-to-volume ratio, incompact porous structure and the small volume of the MWCNTs/chitosan modified paper working zone (Fig. S2 and S3). The immunoreagents diffused only short

distances to react with each other. Furthermore, as the solutions dry in the paper zones, the concentration of each reagent increases; this concentration maybe further enhance the binding kinetics of antibody–antigen (Cheng et al., 2010). Finally, the short incubation times could be favorable to high sample throughput and rapid POCT.

3.3. Evaluation of cross-talk and cross-reactivity

Elimination of the cross-talk between adjacent paper working zones is essential in the multiplexed electrochemical POCT. According to the design of the electrochemical cells on μ PAD (Scheme 1), the diffusion of antigens and signal antibodies from one paper working zone to another should go through two long paper channels and one paper auxiliary zone, and the washing direction could effectively exclude this diffusion. Hence, the possible cross-talk could be avoided. To further confirm the resistance to cross-talk, the cross-reactivity between antigens and non-cognate antibodies was also investigated. For the evaluation of cross-reactivity, this 3D- μ PEID was incubated with the two different capture antibodies for 0.1 U mL^{-1} CA125 and 0.1 ng mL^{-1} CEA, separately, following incubation in the mixture of two trace tag solutions. As expected in Fig. 3, only the paper working zone prepared with corresponding capture antibody showed an obvious DPV response. So the cross-reactivity between antibodies and nonspecific binding at the paper working zones could be eliminated.

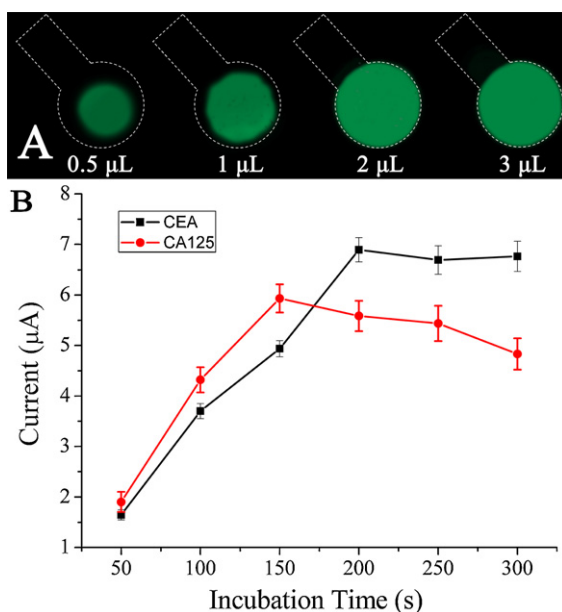


Fig. 2. Parameters affecting DPV responses on this 3D- μ PEID. (A) The pipetting volume affects the uniformity and sufficiency of protein immobilization (4 mm diameter working zones); (B) effects of incubation time on DPV responses at 5 U mL^{-1} CA125 and 5 ng mL^{-1} CEA concentration, where $n=11$ for each point.

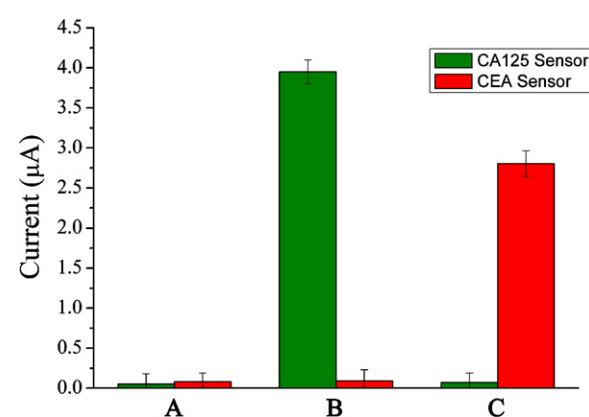


Fig. 3. DPV response for different antigens (0.1 U mL^{-1} CA125 and 0.1 ng mL^{-1} CEA) on different electrodes. (A) Chitosan/MWCNTs modified paper working zone; (B) CA125 antibodies/chitosan/MWCNTs modified paper working zone; (C) CEA antibodies/chitosan/MWCNTs modified paper working zone.

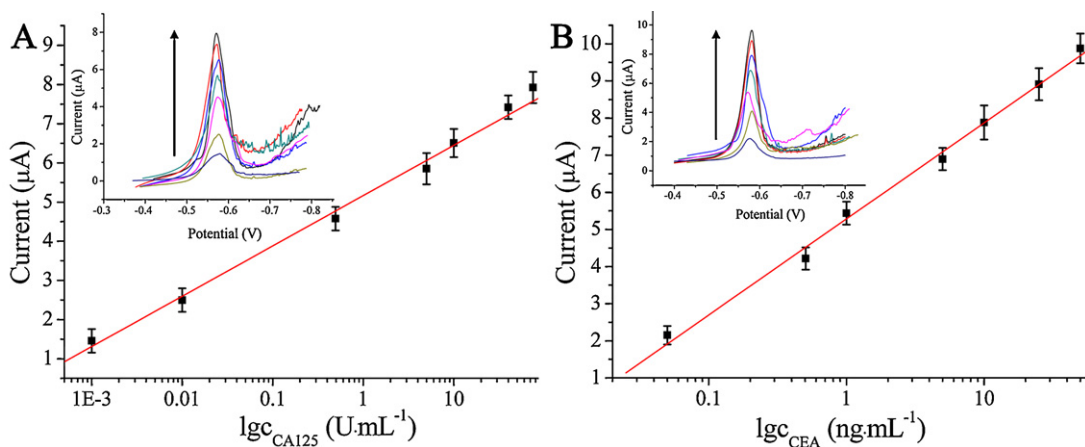


Fig. 4. Calibration curves for CA125 and CEA (eleven measurements for each point). Inset: DPV peaks.

3.4. Analytical performance

Under optimal conditions, the analytical performance of this method was verified by applying 2.0 μ L of samples of human CA125 and CEA standard solutions at various concentrations in 10.0 mM pH 7.4 PBS. Both calibration plots showed good linear relationships between the peak currents and the logarithm values of the analyte concentrations in the range from 0.001 to 75.0 U mL^{-1} for CA125 and 0.05 to 50.0 ng mL^{-1} for CEA that covered most of the levels in human plasmas and serums was also observed (Fig. 4). The linear regression equations were $I = 1.285 \lg c_{\text{CA125}} (\text{U mL}^{-1}) + 5.165$ ($R = 0.9968$), $I = 2.587 \lg c_{\text{CEA}} (\text{ng mL}^{-1}) + 5.283$ ($R = 0.9964$). The limits of detection for CA125 and CEA were 0.2 mU mL^{-1} and 0.01 ng mL^{-1} , respectively, which were lower than 0.28 U mL^{-1} (Wu et al., 2007a), 0.4 U mL^{-1} (Wu et al., 2007b), 0.03 U mL^{-1} (Wu et al., 2008) and 1.2 U mL^{-1} for CA125, and 0.032 ng mL^{-1} (Ho et al., 2009), 1.2 ng mL^{-1} (Wilson, 2005; Wilson and Nie, 2006), 0.45 ng mL^{-1} (Wu et al., 2006), 0.04 ng mL^{-1} (Wu et al., 2008) and 0.19 ng mL^{-1} (Wu et al., 2007a) for CEA reported in previous studies. Thus, on the basis of this standard curve, this 3D- μ PEID should be useful for the determination of the two tumor markers in real serum samples, due to the cutoff values of the two tumor markers in clinical diagnosis are 35 U mL^{-1} and 5 ng mL^{-1} , respectively (Li, 2001).

The analytical reliability and application potential of this 3D- μ PEID was evaluated by assaying clinical serum samples using the proposed method as well as the reference values obtained by commercially used electrochemiluminescence method in Cancer Research Center of Shandong Tumor Hospital. When the levels of tumor markers were over the calibration ranges, serum samples were appropriately diluted with 10.0 mM pH 7.4 PBS prior to assay. The results gave the relative errors less than 5.8% for CA125 and less than 6.5% for CEA, showing an acceptable agreement between the two methods (Table S1). Hence, the developed 3D- μ PEID provided a possible application for the simultaneous detection of Ca125 and CEA in clinical diagnostics.

3.5. Regeneration and reproducibility of this 3D- μ PEID

This 3D- μ PEID could be regenerated for reuse by a simple and effective procedure with the elution reagents, which is very important for the further development of 3D- μ PEID in low-cost application. Furthermore, the regeneration must avoid being harmful to the activity of the immobilized antibodies and damaging the bonds between the antibodies and paper surface when the dissociation of the immunocomplexes occurs (Yakovleva et al., 2003). Different elution reagents were tested using 25 U mL^{-1} CA125 and

25 ng mL^{-1} CEA for regeneration purposes, such as salt solution of organic solvent, high concentration, buffer with low pH value, and diluted alkali solution of different concentrations and pH, were tested. The regeneration efficiencies (REs), proposed by Yakovleva et al. (2002), were calculated according to the following equation.

$$\text{RE} = \left[1 - \frac{RT - B}{T} \right] \times 100\%$$

where, RT represents the DPV response obtained after the regeneration cycle, B is the DPV response for blank, and T is the DPV response before applying any regeneration step. 0.1 M glycine-HCl (pH 2.1) showed the best regeneration efficiency at more than 96% for these two tumor markers, which was chosen as the elution reagent for the regeneration of this 3D- μ PEID. With the regeneration procedure, this 3D- μ PEID could be used for ten cycles with an acceptable reproducibility.

The relative standard deviation (RSD), using CEA as a model, for ten parallel measurements on the same one paper working zone (intraassay) incubated with the incubation solution containing 25 ng mL^{-1} CEA was 5.87%, indicating a good precision. The detections of 25 ng mL^{-1} CEA on ten different paper working zones fabricated independently (interassay) showed a RSD of 4.21%, giving an acceptable fabrication reproducibility of this 3D- μ PEID.

When this 3D- μ PEID was stored dry at 4 °C (sealed) and measured at intervals of 3 days, no obvious change was observed after storing for 4 weeks, indicating that this 3D- μ PEID was stable for storage or long-distance transport in remote regions and developing countries.

4. Conclusion

Using CA125 and CEA as model, a novel 3D- μ PEID was demonstrated. Microfluidic paper-based analytical devices are (1) exceedingly inexpensive, (2) easily fabricated for rapid prototyping of new designs, (3) made from abundant raw materials, (4) conveniently incinerated for rapid disposal of hazardous waste and (5) stand-alone devices that do not require external pumps or other complicated equipment to move fluids. These advantages make this 3D- μ PEID an innately exciting platform for building a new generation of simple, low-cost, disposable and portable point-of-care diagnostic devices with analytical characteristics that eventually may surpass polymer-based microfluidic devices. The immobilization of antibodies on the MWCNTs/chitosan modified working zones was very useful for performing high-performance sandwich electrochemical immunoassay by enhancing the conductivity of working zones and stability of antibodies on paper. The proposed 3D- μ PED in this work has combined the simplicity

and low-cost of μ PADs and the sensitivity and selectivity of electrochemical immunoassay. This proposed MWCNTs/chitosan modified 3D- μ PEID will be very useful when the level of an analyte in real biological sample is very important for simple, rapid, low-cost point-of-care testing in remote regions, developing or developed countries.

Moreover, this novel 3D- μ PED fabrication strategy cannot only be used for fabrication of paper-based electrochemical immunodevice, but also to fabricate paper-based electrochemical enzyme device and paper-based electrochemical DNA device based on the covalent immobilization of enzyme and DNA molecules on working electrode. Finally, although the demonstrated assay used electrochemistry as the reporting mechanism, this 3D- μ PID can also be combined with electrochemiluminescence and photoelectrochemistry assay using corresponding signal antibodies.

Acknowledgments

This work was financially supported by Natural Science Research Foundation of China (21175058), Natural Science Foundation of Shandong Province, China (ZR2011BQ019) and Technology Development Plan of Shandong Province, China (grant no. 2011GGB01153).

Appendix A. Supplementary data

Supplementary data associated with this article can be found, in the online version, at doi:10.1016/j.bios.2011.12.021.

References

- Abe, K., Suzuki, K., Citterio, D., 2008. *Anal. Chem.* 80, 6928.
- Apilux, A., Dungchai, W., Siangproh, W., Praphairaksit, N., Henry, C.S., Chailapakul, O., 2010. *Anal. Chem.* 82, 1727.
- Carrilho, E., Martinez, A.W., Whitesides, G.M., 2009b. *Anal. Chem.* 81, 7091.
- Carrilho, E., Phillips, S.T., Vella, S.J., Martinez, A.W., Whitesides, G.M., 2009a. *Anal. Chem.* 81, 5990.
- Carvalhal, R.F., Simão Kfouri, M., de Oliveira Piazetta, M.H., Gobbi, A.L., Kubota, L.T., 2010. *Anal. Chem.* 82, 1162.
- Cheng, C.-M., Martinez, A.W., Gong, J., Mace, C.R., Phillips, S.T., Carrilho, E., Mirica, K.A., Whitesides, G.M., 2010. *Angew. Chem. Int. Ed.* 49, 4771.
- Chitnis, G., Ding, Z., Chang, C.-L., Savran, C.A., Ziae, B., 2011. *Lab Chip* 11, 1161.
- Delaney, J.L., Hogan, C.F., Tian, J., Shen, W., 2011. *Anal. Chem.* 83, 1300.
- Dungchai, W., Chailapakul, O., Henry, C.S., 2009. *Anal. Chem.* 81, 5821.
- Fenton, E.M., Mascarenas, M.R., López, G.P., Sibbett, S.S., 2009. *ACS Appl. Mater. Interfaces* 1, 124.
- Ho, J.A., Lin, Y.-C., Wang, L.-S., Hwang, K.-C., Chou, P.-T., 2009. *Anal. Chem.* 81, 1340.
- Hwang, H., Kim, S.-H., Kim, T.-H., Park, J.-K., Cho, Y.-K., 2011. *Lab Chip* 11, 3404.
- Li, T.X., 2001. *Modern Clinical Immunoassay*, 1st ed. Military Medical Science Press, Beijing.
- Li, X., Tian, J., Nguyen, T., Shen, W., 2008. *Anal. Chem.* 80, 9131.
- Lu, Y., Shi, W., Qin, J., Lin, B., 2009. *Anal. Chem.* 82, 329.
- Martinez, A.W., Phillips, S.T., Butte, M.J., Whitesides, G.M., 2007. *Angew. Chem. Int. Ed.* 46, 1318.
- Martinez, A.W., Phillips, S.T., Nie, Z., Cheng, C.-M., Carrilho, E., Wiley, B.J., Whitesides, G.M., 2010b. *Lab Chip* 10, 2499.
- Martinez, A.W., Phillips, S.T., Whitesides, G.M., 2008b. *PNAS* 105, 19606.
- Martinez, A.W., Phillips, S.T., Whitesides, G.M., 2010a. *Anal. Chem.* 82, 3.
- Martinez, A.W., Phillips, S.T., Wiley, B.J., Gupta, M., Whitesides, G.M., 2008a. *Lab Chip* 8, 2146.
- Nie, Z., Deiss, F., Liu, X., Akbulut, O., Whitesides, G.M., 2010a. *Lab Chip* 10, 3163.
- Nie, Z., Nijhuis, C.A., Gong, J., Chen, X., Kumachev, A., Martinez, A.W., Narovlyansky, M., Whitesides, G.M., 2010b. *Lab Chip* 10, 477.
- Noh, H., Phillips, S.T., 2010. *Anal. Chem.* 82, 4181.
- Ornatska, M., Sharpe, E.M., Andreescu, D., Andreescu, S., 2011. *Anal. Chem.* 83, 4273.
- Osborn, J.L., Lutz, B., Fu, E., Kauffman, P., Stevens, D.Y., Yager, P., 2010. *Lab Chip* 10, 2659.
- Sia, S.K., Kricka, L.J., 2008. *Lab Chip* 8, 1988.
- Tobjörk, D., Österbacka, R., 2011. *Adv. Mater.* 23, 1935.
- Wang, S., Ge, L., Song, X., Yu, J., Ge, S., Huang, J., Zeng, F., 2012. *Biosens. Bioelectron.* 31, 212.
- Whitesides, G.M., 2011. *Lab Chip* 11, 191.
- Wilson, M.S., 2005. *Anal. Chem.* 77, 1496.
- Wilson, M.S., Nie, W., 2006. *Anal. Chem.* 78, 6476.
- Wu, J., Tang, J., Dai, Z., Yan, F., Ju, H., Murr, N.E., 2006. *Biosens. Bioelectron.* 22, 102.
- Wu, J., Yan, F., Tang, J., Zhai, C., Ju, H., 2007a. *Clin. Chem.* 53, 1495.
- Wu, J., Yan, Y., Yan, F., Ju, H., 2008. *Anal. Chem.* 80, 6072.
- Wu, J., Zhang, Z., Fu, Z., Ju, H., 2007b. *Biosens. Bioelectron.* 23, 114.
- Yáñez-Sedeno, P., Pingarrón, J.M., Riu, J., Rius, F.X., 2010. *TrAC, Trends Anal. Chem.* 29, 939.
- Yakovleva, J., Davidsson, R., Bengtsson, M., Laurell, T., Emnéus, J., 2003. *Biosens. Bioelectron.* 19, 21.
- Yakovleva, J., Davidsson, R., Lobanova, A., Bengtsson, M., Eremin, S., Laurell, T., Emnéus, J., 2002. *Anal. Chem.* 74, 2994.
- Yu, J., Ge, L., Huang, J., Wang, S., Ge, S., 2011. *Lab Chip* 11, 1286.
- Zhao, J., Henkens, R.W., Stonehuerer, J., O'Daly, J.P., Crumbliss, A.L., 1992. *J. Electroanal. Chem.* 327, 109.

Paper-based Three-dimensional Electrochemical Immunodevice based on Multi-walled Carbon Nanotubes Functionalized Paper for Sensitive Point-of-care Testing

Panpan Wang^a, Lei Ge^a, Xianrang Song^b, Mei Yan^a, Shenguang Ge^c, Jinghua Yu^{*a}

^aSchool of Chemistry and Chemical Engineering, University of Jinan, Jinan 250022, P.R. China

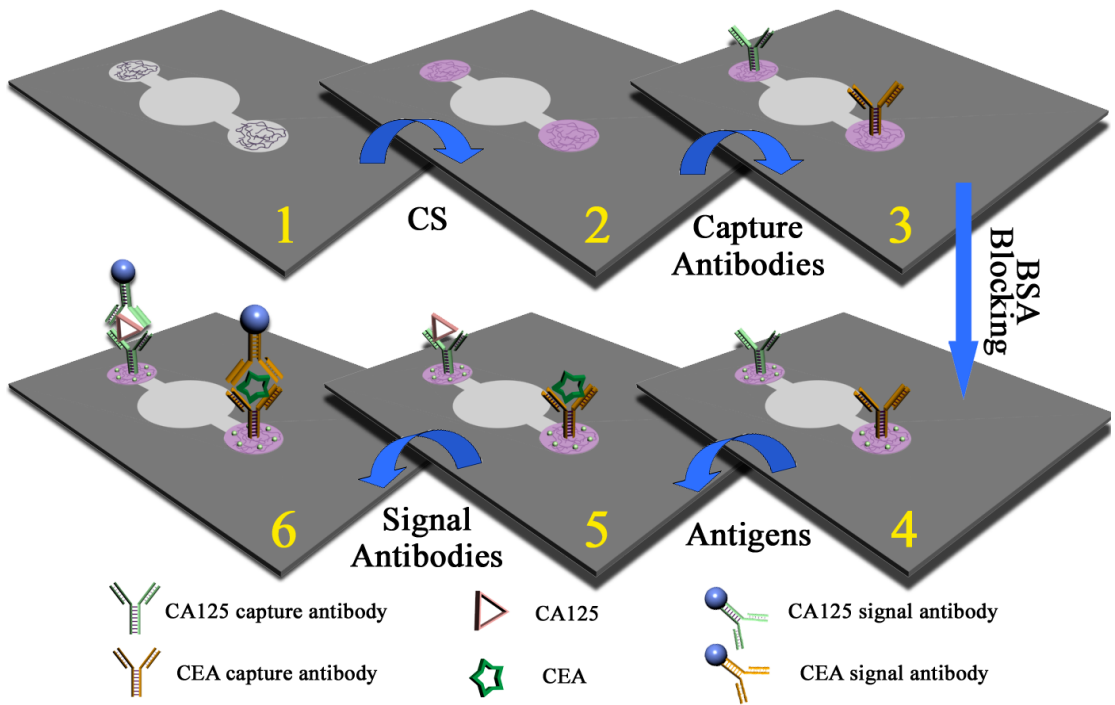
^bCancer Research Center, Shandong Tumor Hospital, Jinan 250117, P.R. China

^cShandong Provincial Key Laboratory of Fluorine Chemistry and Chemical Materials, University of Jinan, Jinan 250022, P.R. China

Supplemental Information

Pretreatments of MWCNTs and chitosan

The MWCNTs were firstly treated with 3:1 H₂SO₄/HNO₃ under sonication for 4 h to shorten the MWCNTs, remove metallic and carbonaceous impurities, and generate carboxylate groups on the MWCNTs surfaces (Lai et al., 2009). The resulting MWCNTs were separated and washed repeatedly with distilled water by centrifugation until the pH 7 was reached. A 0.25 mg·mL⁻¹ chitosan stock solution was prepared by dissolving chitosan flakes in hot (80~90 °C) aqueous solution with 0.05 M HCl. After the solution was cooled to room temperature, the pH was adjusted to 3.5~5.0 with NaOH solution. The chitosan solutions were filtered using a 0.45 μm Millex-HA syringe filter unit (Millipore) and stored in a refrigerator (4 °C) when not in use.



Scheme S1 Schematic representation of the fabrication and assay procedure for this 3D- μ PEID. 1) wax-patterned paper layer after MWCNTs modification; 2) after chitosan/MWCNTs modification; 3) after capture antibody/chitosan/MWCNTs modification; 4) after blocking and washing; 5) after capturing and washing; 6) after incubation with signal antibodies and washing.

Detail washing procedure for this 3D- μ PID

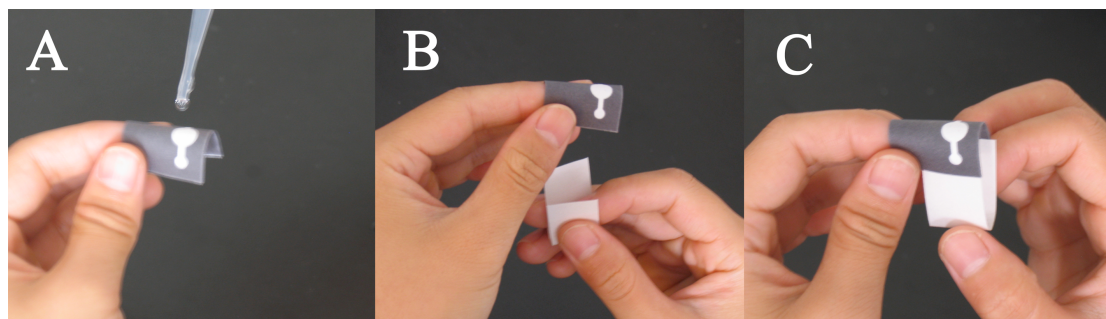


Figure S1 Pictures of the washing procedures for this 3D- μ PID. A) Adding PBS or washing buffer to the back of the paper auxiliary zone while bending the paper to a inverted-U type; B, C) Contacting the two paper working zones with a piece of U-type blotting paper.

The detailed washing procedures was as follows: Due to the front and back surfaces of the wax-patterned paper electrochemical cell on paper layer are open to atmosphere, thus the working zone can be washed by adding PBS or washing buffer to the back of the paper auxiliary zone while bending the paper layer to a inverted-U type as shown in Figure S1A. Then a piece of U-type blotting paper was contacted with the two paper working zones simultaneously (Figure S1B, C). The washing buffer goes through the paper and migrates along the paper channels by the capillary and gravity action to wash the paper channels and paper working zones and carries the unbound reagents with it into the blotting paper. This effective washing procedure was used in this work consistently and acquiescently. The washing process was important for preventing the nonspecific binding and for achieving the best possible signal-to-background ratio. Another purpose for this washing procedure was to stop the incubation reaction at exactly same time.

Characterizations of this 3D- μ PEID

This 3D- μ PEID was fabricated on pure cellulose paper (Figure S2A and Figure S3A). The hydrophilic electrochemical cell was fabricated by printing wax on the paper surface in a high-resolution printing mode (Figure S2B). Owing to the 3D porous structure of paper, the melted wax can penetrate into the paper to decrease the hydrophilicity of paper remarkably (Figure S2C). After the curing process, the printed area sustains an apparent contact angle for water of 124°. And the unprinted area maintains good hydrophilicity, flexibility and 3D porous structure and will not affect the further modification of the paper working zones.

The modification of the paper working zones in paper electrochemical cell is an important factor affecting the sensing performance of this 3D- μ PEID. The morphologies of MWCNTs modified paper working zone, chitosan/MWCNTs modified paper working zone and antibodies/chitosan/MWCNTs modified paper working zone were characterized by SEM. Figure S3B, C exhibits that MWCNTs were mostly assembled on cellulose fibers through physical adsorption in the form of small bundles or single tubes. The uniform nanostructure can significantly increase the effective surface of the screen-printed electrode indirectly after stacking for loading of biomolecules and accelerating the rate of electron transfer. In comparison with the pure cellulose fibers (Figure S3A), the morphology of chitosan coated MWCNTs modified cellulose fibers (Figure S3D, E) displayed more stable assembly surface which was advantageous to improve the reproducibility of immunodevice preparation. After antibodies immobilization, paper working zones still showed an incompact porous structure (Figure S3F), which can facilitate the approach of immunoreagents to the immobilized antibodies and access of the substrate to its corresponding enzyme and resulted in fast immunoreaction and sensitive electrochemical

response.

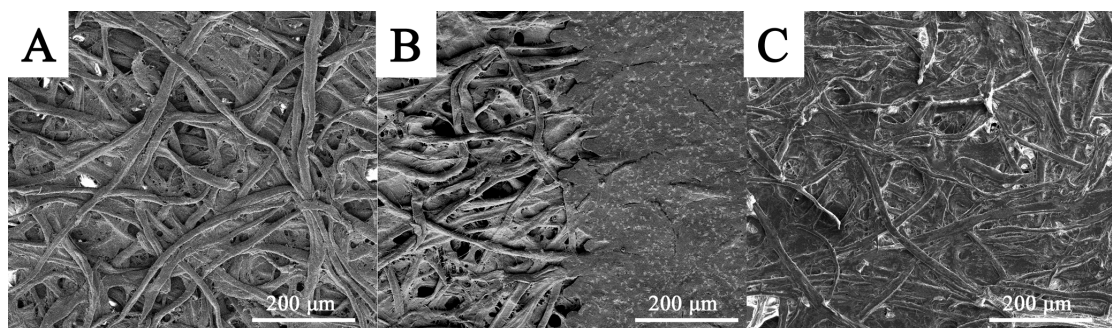


Figure S2. SEM images of A) pure cellulose paper; B) the boundary of wax-pattern: left is pure paper, right is wax-printed paper. C) surface of wax-penetrated paper.

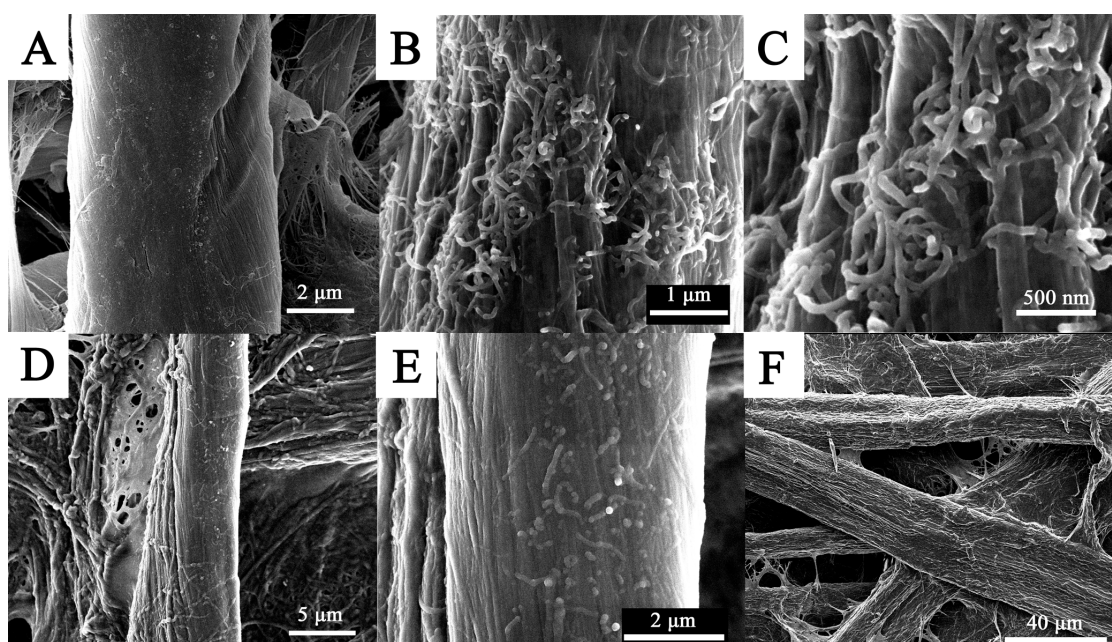


Figure S3. SEM images of A) pure cellulose paper; B) MWCNTs assembled paper; C) enlarged image of B); D) chitosan/MWCNTs modified paper; E) enlarged image of D); F) antibodies/chitosan/MWCNTs modified paper.

The electrochemical impedance spectroscopy (EIS) of the resulting paper working zones could give further information on the assembly process shown in Scheme S1. In this work, the $[Fe(CN)_6]^{3-/-4-}$ redox couple is used to characterize the 3D- μ PEID feature in electrochemistry. The electron transfer of $[Fe(CN)_6]^{3-/-4-}$ can be blocked by the formation of BSA/antibody/chitosan/MWCNTs composites in the paper working zone, which results in an increase of the electron transfer resistance. Figure S4 shows the Nyquist plots of EIS observed upon the stepwise modification processes. The original paper working zone on the μ PAD revealed

a small semicircle domain (Figure S4, curve a), which implied a low-electron-transfer resistance of the redox couple. After MWCNTs was assembled on the μ PAD, the resistance was decreased (Figure S4, curve b), for the existence of the MWCNTs leads to the increase of the electron transfer kinetics of $[\text{Fe}(\text{CN})_6]^{3-/4-}$ and the effective conductive gap to the electrode/paper interface. It could be found that chitosan modified μ PAD showed a much lower resistance for the redox probe (Figure S4, curve c), the reason of which may be the abundant amino groups can adsorb much more negatively charged $[\text{Fe}(\text{CN})_6]^{3-/4-}$ and it can be easily reached at the fiber surface to accelerate electron transfer. However, for the antibody modified μ PAD through glutaraldehyde linking, the diameter increased markedly (curve d in Figure S4), which can be accounted for the association of glutaraldehyde with chitosan obturated many amino groups of chitosan and formation of protein barrier for electron transfer. Similarly, BSA could also resist the electron-transfer kinetics of the redox probe at the paper interface, resulting in the increasing impedance of the paper working zone (curves e), which testified the immobilization of BSA.

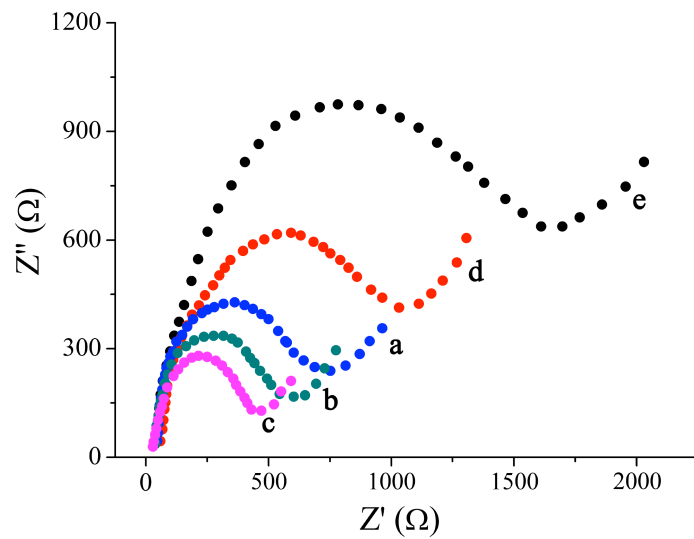


Figure S4. EIS of original (a); MWCNTs modified (b); chitosan/MWCNTs modified (c); capture-antibody/GA/chitosan modified paper working zone before (d) and after (e) blocking with BSA in 0.1 M KCl containing 5.0 mM $[\text{Fe}(\text{CN})_6]^{3-}$ and 5 mM $[\text{Fe}(\text{CN})_6]^{4-}$.

Figure S5 shows recorded cyclic voltammograms of the

MWCNTs/chitosan/glutaraldehyde/capture antibodies/BSA modified paper working zone containing 10.0 mM PBS (2 mM $[Fe(CN)_6]^{3-/-4-}$ and 0.1 M KCl, pH 7.4) at different scan rates. It can be observed the peak current increased and the peak potential shifted slightly. As shown in the inset of Figure S5 in the scan rate range of 10-100 mV·s⁻¹, the peak currents became proportional to the square root of the scan rate, showing a diffusion-controlled process.

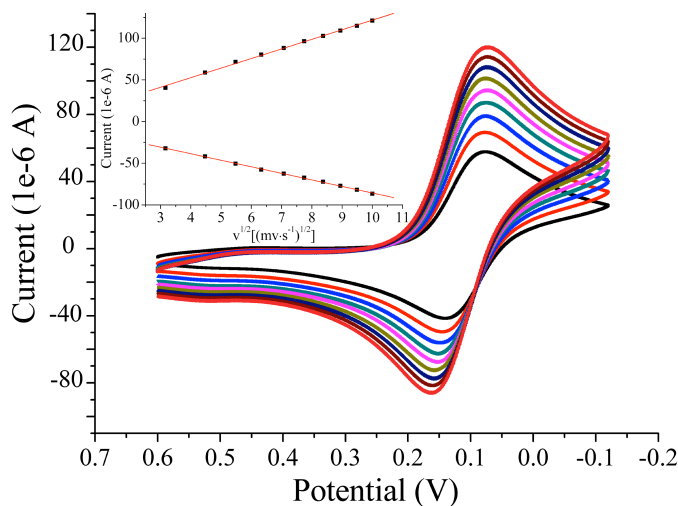


Figure S5. Cyclic voltammograms of MWCNTs/chitosan/glutaraldehyde/capture antibodies/BSA modified paper working zone in 10.0 mM pH 7.4 PBS (2 mM $[Fe(CN)_6]^{3-/-4-}$ and 0.1 M KCl, pH 7.4) at 10, 20, 40, 50, 60, 80, 90 and 100 mV·s⁻¹ (from inner to outer). Inset: plots of peak current vs. $v^{1/2}$.

Table S1. Assay results of real human serum by the proposed and reference method

Analytes	CA125 ($U \cdot mL^{-1}$)			CEA ($ng \cdot mL^{-1}$)		
	Sample 1	Sample 2	Sample 3	Sample 1	Sample 2	Sample 3
Proposed method*	63.58	40.75	4.07	3.20	9.41	38.62
Reference method*	60.11	41.61	3.90	3.31	9.08	41.31
Relative error (%)	5.77	-2.07	4.36	-3.32	3.63	-6.51

* Average of eleven measurements.

Procedures of the optimization of pipetting volume

Thus, FITC-labeled CEA capture antibodies were used as a model to investigate the optimum pipetting volume of solutions onto each paper working zone. The investigation procedures included (i) immobilization of the FITC-labeled CEA capture antibodies with different volumes on the MWCNTs/chitosan modified paper working zone through glutaraldehyde cross-linking on μ PAD; (ii) then the paper working zones were washed twice following the procedure mentioned above; (iii) the fluorescence images of the paper channels and paper working zones were investigated on an inverse fluorescence microscope (ChangFang CFM-500E, China).

Reference

Lai, G.S., Yan, F., Ju, H.X., 2009. Anal. Chem. 81, 9730.